AD-A069 867 TEXAS INST FOR COMPUTATIONAL MECHANICS AUSTIN F/G 12/1
GALERKIN AND COLLOCATION-GALERKIN METHODS WITH SUPERCONVERGENCE--ETC(U)
JUN 79 G F CAREY, D HUMPHREY, M F WHEELER N00014-78-C-0550

UNCLASSIFIED TR-1 NL

| OF |
AD
A069867

END
DATE
FILMED
7 -79
DDC

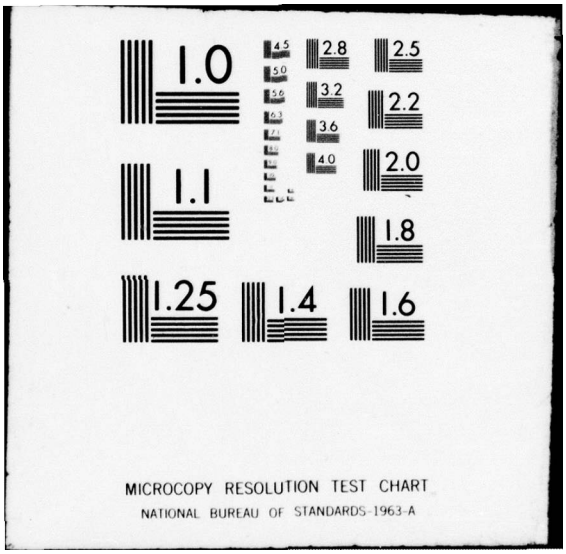
1.0
1.1
1.25
1.4
1.6
1.8
2.0
2.2
2.5
2.8
3.2
3.6
4.0
4.5
5.0
5.6
6.3
MICROCOPY RESOLUTION TEST CHART
NATIONAL BUREAU OF STANDARDS-1963-A

GALERKIN AND COLLOCATION-GALERKIN METHODS WITH SUPERCONVERGENCE AND OPTIMAL FLUXES

G. F. Carey[1], D. Humphrey[2], M. F. Wheeler[3]

(Submitted to International Journal of Numerical Methods in Engineering)

1 Texas Institute for Computational Mechanics, University of Texas, Austin, Texas.

2 Lawrence Livermore Laboratories, Livermore, California.

3 Mathematical Sciences Dept., Rice University, Houston, Texas.

DISCLAIMER NOTICE

THIS DOCUMENT IS BEST QUALITY PRACTICABLE. THE COPY FURNISHED TO DDC CONTAINED A SIGNIFICANT NUMBER OF PAGES WHICH DO NOT REPRODUCE LEGIBLY.

TABLE OF CONTENTS

LIST OF FIGURES

LIST OF TABLES

GALERKIN AND COLLOCATION-GALERKIN METHODS WITH SUPERCONVERGENCE AND OPTIMAL FLUXES

G. F. Carey[1], D. Humphrey[2], M. F. Wheeler[3]

ABSTRACT

Finite element methods are formulated and investigated for the effectiveness factor problem for heat and mass transfer with chemical reactions in catalyst pellet models. A Galerkin finite element method is compared with a previous C^1 collocation method ([7], 1975). A scheme that is conceptually intermediate between these two methods and accordingly has been termed collocation-Galerkin is formulated and numerical experiments considered. Of particular interest here are superconvergence results at the Gauss and Jacobi points, respectively. Numerical studies of superconvergence in the presence of a nonlinear reaction-rate term are presented. An integral formula is devised and used to compute the flux at the pellet surface to optimal accuracy. Numerical experiments are conducted to demonstrate the improvement in computed fluxes.

INTRODUCTION

The particular class of nonlinear two-point boundary problems considered here arise in describing heat and mass transfer in a catalyst pellet with accompanying chemical reaction. Such problems are of considerable importance in the study of packed bed reactors in chemical engineering where the catalyst

---

1 Texas Institute for Computational Mechanics, University of Texas, Austin, Texas.

2 Lawrence Livermore Laboratories, Livermore, California.

3 Mathematical Sciences Dept., Rice University, Houston, Texas.

pellets constitute the solid phase. The complexity of transport processes for both fluid and solid phases in the reactor lead to "separation" of the problem to computations in the solid and fluid, respectively. Moreover, since the characteristic local rates in the pellet are large relative to those for the reactor, a steady-state model for heat and mass transfer in the pellet can be assumed [1,2,3].

In practical simulations of transient models for chemical reactors the catalyst-pellet problem may require solution numerous times. Moreover, the form of solution may be quite sensitive to the choice of reaction rate parameters such as Thiele modulus and there may be bifurcations with multiple solutions. Consequently, numerical solution may be a formidable task for certain parameter ranges. The model is capable of representing both relatively quiescent solutions where the reaction rate is small, and also "ignited" states where the reaction rate is high in the vicinity of the pellet surface and a boundary-layer results.

For these reasons a variety of numerical methods have been developed for solving the associated nonlinear two-point problems. Global residual methods, particularly collocation methods, have been devised and extensively used. Of these methods global orthogonal collocation methods provide optimal accuracy and efficient solution for effectiveness factor problems with low-to-moderate and even quite large Thiele modulus. Excellent treatments of the theory and techniques and numerous examples are described in the recent literature [4,5].

If the Thiele modulus is large and the solution has a steep gradient near the pellet surface the global orthogonal collocation method, and global expansion methods in general, are not appropriate. The polynomial degree must be high to ensure that there are sufficient points in the boundary-layer

zone. This, in turn, leads to concommitant errors due to ill-conditioning of the nonlinear algebraic problem and also to convergence problems in iterative solution algorithms. Essentially, these global methods attempt to determine a very smooth solution to problems where the exact solution may have discontinuous or large derivatives. One approach to the problem with large Thiele modulus introduces a "burnt out" region which the solution is zero and a "reaction layer" and the problem is solved in the reaction layer by orthogonal collocation [6].

In a previous paper [7] the method of orthogonal collocation on finite elements is developed to combine the accuracy of orthogonal collocation within a finite element framework. This naturally allows graded nonuniform meshes which are coarse in the pellet interior and fine in the boundary layer. The particular scheme applied is a C^1 collocation method with polynomial approximation on each element and, naturally, continuity of function and derivative only at the element interfaces.

C^0-Galerkin techniques presently constitute the most widely analysed and applied class of finite element methods for two-point problems and elliptic boundary-value problems (for example, see [8]-[11]). Superconvergence estimates of the Galerkin and collocation methods have been proven for linear two-point problems with smooth coefficients [12,14,22]. In the early sections of this paper we formulate and apply the C^0-Galerkin finite element method for the nonlinear pellet problem, addressing in particular the superconvergence properties in the presence of the nonlinearity.

The C^1 collocation formulation requires no quadratures and this may lead to more efficient computations than Galerkin methods, especially when iterative solution is required and the computation in the pellet is coupled with a transient time-stepping solution in the fluid phase. On the other

hand, the C^0-Galerkin method while necessitating element quadrature computations, requires only continuity of the approximant. Thus, the Galerkin methods are better able to treat discontinuities, layers and other irregular solution behavior. We combine some of the efficiency and simplicity of C^1 collocation with the lower continuity of C^0-Galerkin in an intermediate method, here termed C^0-Collocation-Galerkin. Error estimates for such "weak" methods and linear problems are presented in [15]. The C^0-Galerkin method is superconvergent at the nodes (knows). For linear problems the C^0-Collocation-Galerkin method is superconvergent at the nodes (knots) if the Jacobi points are collocation points and we give here the theoretical superconvergence estimates for linear and nonlinear reaction rate terms with accompanying numerical studies of convergence and accuracy [16].

The flux at the catalyst boundary is of practical importance and a special quadrature technique is applied on the extreme element at the boundary to compute the flux to optimal accuracy. Numerical results for the boundary flux are compared with those obtained by more standard approaches.

PART I. GALERKIN METHOD, SUPERCONVERGENCE AND FLUX CALCULATIONS

Galerkin Finite Element Method

We describe briefly the standard Galerkin finite element method prior to considering details concerning superconvergence. This also facilitates subsequent description of the C^0-Collocation-Galerkin method.

Consider the diffusion and reaction of a species in an isothermal catalyst pellet as described by the equation

$$\frac{1}{x^{a-1}} \frac{d}{dx} \left(x^{a-1} \frac{dc}{dx}\right) = f(c) \quad , \quad 0 < x < 1 \tag{1}$$

with

$$\frac{dc}{dx}(0) = 0 \quad \text{and} \quad -\frac{dc}{dx}(1) = Bi_m(c(1) - 1) \tag{2}$$

where a = 1,2 or 3 for planar, cylindrical and spherical geometry, Bi_m is the Biot number for mass transfer [1], and f(c) is the reaction rate expression for the problem in consideration.

Introduce an approximation c(x) into the differential equation to determine the residual. On applying the weighted residual condition, the usual integration by parts yields the (weak) variational statement of the problem,

$$-\int_0^1 x^{a-1}(c'(x)v'(x) + f(c)v)dx + x^{a-1}c'(x)v(x)\Big|_0^1 = 0 \tag{3}$$

for admissible test functions v(x) and where the "prime" denotes differentiation.

In a C^0-Lagrange finite element method the approximation on a partition of m elements and having n nodes $x_1 = 0 < x_2 < \ldots < x_n = 1$, has the form

$$c(x) = \sum_{j=1}^{n} c_j \phi_j(x) \tag{4}$$

where $\{\phi_j(x)\}$ are piecewise-polynomial patch functions associated with the nodes $\{j\}$ of the mesh. In the simplest instance, $\phi_j(x)$ is linear on each element and satisfies $\phi_j(x_i) = \delta_{ij}$, Kronecker delta.

The Galerkin method utilizes the same test space as trial space so that $v(x) = \{\phi_i(x)\}$, $i = 1,\ldots,n$ and from equation (3),

$$\sum_{j=1}^{n} \left(\int_0^1 x^{a-1} \phi_i' \phi_j' dx \right) c_j = - \int_0^1 x^{a-1} \phi_i f(c) dx + c'(1)\phi_i(1) \quad ,$$

$$i,j = 1,2,\ldots,n \tag{5}$$

whence from (2),

$$\sum_{j=1}^{n} \left(\int_0^1 x^{a-1} \phi_i' \phi_j' dx \right) c_j + Bi_m c_n \delta_{in} + \int x^{a-1} \phi_i f(c) dx = Bi_m \delta_{in}$$

$$i,j = 1,2,\ldots,n \tag{6}$$

For convenience, we write this in matrix form as

$$\underset{\sim\sim}{A}\underset{\sim}{c} + \underset{\sim}{F}(\underset{\sim}{c}) = \underset{\sim}{b} \quad \text{or} \quad \underset{\sim}{g}(\underset{\sim}{c}) = \underset{\sim}{0} \tag{7}$$

where the vector $\underset{\sim}{F}(\underset{\sim}{c})$ represents the contribution of the nonlinear reaction rate term to the finite element system and, clearly, $\underset{\sim}{g}(\underset{\sim}{c}) = \underset{\sim\sim}{A}\underset{\sim}{c} + \underset{\sim}{F}(\underset{\sim}{c}) - \underset{\sim}{b}$.

Considering a general element e of degree k with end nodes x_r and x_s, $(s = r + k)$, the element contributions to the nonlinear system (7) are

$$(a_{ij})_e = \int_{x_r}^{x_s} x^{a-1} \ell_i'(x) \ell_j'(x) dx$$

and

$$i,j = 1,2,\ldots,k+1 \tag{8}$$

$$(f_i)_e = \int_{x_r}^{x_s} x^{a-1} \ell_i(x) f(c) dx$$

where $\{\ell_i(x)\}$ are the local Lagrange polynomials of degree k on element e,

$\ell_i(x_j) = \delta_{ij}$ on $\Omega_e = [x_r, x_s]$.

Remark: The above formulation is quite standard and can be readily generalized to finite element bases other than those of Lagrange type [10,11]. We shall utilize these and similar relations for subsequent superconvergence, flux and Collocation-Galerkin derivations.

Nonlinear System Solution

Depending on the strength of the nonlinear reaction rate term, either of two iterative techniques are applied. For mildly nonlinear problems a Picard (successive approximation) iteration is suitable. For iterate k+1,

$$\underset{\sim}{A}\underset{\sim}{c}^{k+1} = \underset{\sim}{b} - \underset{\sim}{F}(\underset{\sim}{c}^{k}) \quad , \qquad k = 0,1,... \tag{9}$$

This iteration fails at large Thiele modulus and a Newton iteration is used,

$$\underset{\sim}{J}(\underset{\sim}{c}^{k+1} - \underset{\sim}{c}^{k}) = -\underset{\sim}{g}(\underset{\sim}{c}^{k}) \quad , \qquad k = 0,1,... \tag{10}$$

Details concerning the structure of the Jacobian $\underset{\sim}{J}$ and system matrix $\underset{\sim}{A}$, efficient direct solution by blocks and element block storage are similar to those described in the previous study of orthogonal collocation on finite elements [7] and will not be elaborated upon here. One important distinction is that $\underset{\sim}{J}$ and $\underset{\sim}{A}$ are now symmetric, a feature that is exploited in the solution algorithms.

Error Estimates

Let $\hat{c}(x)$ denote the exact solution and $e(x) = \hat{c}(x) - c(x)$ the error. We introduce an inner product with weight factor x^{a-1} and the associated normed spaces J^m which are the closure of C^∞ functions with respect to the weighted m-norm,

$$\| u \|_m = \left(\sum_{j=0}^{m} \| u^{(j)} \|^2 \right)^{1/2} \tag{11}$$

where $\| f \|_\Omega^2 = \int x^{a-1} f^2 \, dx$ defines the weighted norm.

For a linear reaction term the standard error estimates follow even for the singular differential equation [17],

$$\| e \|_B \leq C h^m \| \hat{c}^{(m)} \|_B \tag{12}$$

where B is the unit "ball" in the domain, and h is the element length.

The global weighted norm of the error in the derivative is $O(h^{m-1})$ as expected [10,17].

Remark: For a spherical pellet ($a = 3$) the transformation $u = xc$ yields a nonsingular equation and the standard L_2 norms can be used to obtain

$$\| e^{(j)} \| \leq C h^{m-j} \| u \|_{m,\Omega} , \quad j = 0,1,\ldots,m \tag{13}$$

where $\Omega = [0,1]$.

Let the reaction rate expression be nonlinear with f and $\partial f/\partial u$ continuous on $x \in [0,1]$, $c \in [-\infty, \infty]$. Furthermore, let $\left| \frac{\partial f}{\partial u} (x,u) \right| \leq M$ for all x,u as above and

$$\frac{\partial f}{\partial u} (x,u) \leq \lambda < \Lambda \tag{14}$$

where Λ is the minimum eigenvalue of the generalised eigenproblem for the differential operator. Then [9] if $u \in C^m$ and the differential operator is strongly coercive we again obtain the bounds of (13) for the nonlinear reaction in a spherical catalyst pellet.

Thus, to obtain global error estimates for mass transfer with nonlinear reaction in a spherical catalyst pellet we require bounds on the derivative $\partial f/\partial c$ of the nonlinear term. This implies that for mildly nonlinear problems we should obtain the global rates indicated but that the rates have not been established theoretically for problems with boundary-layers that are very

pronounced.

Superconvergence

For linear problems there are special points within the elements at which the approximation is much more accurate than the global rates suggest. If $p(x) = 1$ and $q(x) = 0$ the approximate solution is exact at the nodes and for more general linear differential equations one can prove that the solution or its derivatives are locally very accurate at special points such as the Gauss or Jacobi points [12]. In the case of the C^0 Galerkin method the solution is superconvergent at the nodes (knots) and the derivative is superconvergent at the Gauss points, whereas in the previous C^1 collocation investigations the solution is superconvergent at the Gauss points [7]. The following numerical studies are designed to investigate superconvergence for the class of practical catalyst models described earlier.

We first consider the problem of equation (1)-(2) with $Bi_m \to \infty$ so that the boundary condition becomes $c(1) = 1$. On a spherical domain and with small Thiele modulus we obtain a smoothly varying, almost parabolic solution. The nonlinear reaction rate term

$$f(c) = \phi^2 c \exp[\gamma(1-1/T)] \quad , \qquad T = 1 + \beta - \beta c \tag{15}$$

corresponds to an irreversible, first-order, non-isothermal reaction and parameters $\phi = 0.8$, $\gamma = 18$, $\beta = 0.3$ are chosen. The choice $\phi = 0.8$ for the Thiele modulus yields a concentration profile that varies from approximately 0.7 at $x = 0$ to 1.0 at $x = 1$. At smaller ϕ values the solution changes very slowly and it is difficult to display the superconvergence results effectively for finite precision computations.

From the linear theory we anticipate that, at least for moderate nonlinearities of the type indicated above, globally the finite element solution on a uniform mesh should be $O(h^{k+1})$ accurate and the derivative $O(h^k)$, where

k is the degree of the element polynomial - with piecewise linear these L_2 error estimates are $O(h^2)$ and $O(h)$, respectively. Since the derivative c' is superconvergent at the Gauss points in the linear problem, we now look for $O(h^2)$ at these points in the nonlinear catalyst model. As the Gauss points are to be interrogated for superconvergent derivatives, a set of nested mesh refinements is designed such that specific Gauss points are common Gauss points to all the meshes. This implies that the element basis for these numerical experiments be of odd degree and that in successive nested refinements each element be split to an odd number of elements. In this way the central Gauss point of an element is preserved through successive refinements.

Using an initial mesh of 5 elements and a piecewise linear basis, the errors in solution and derivative at the Gauss points (0.1,0.3,...,0.9) are computed and monitored in Table 1 for successive meshes of 25, 125 and 625 elements. The derivative values computed from a mesh of 1250 elements are taken as exact to ten decimal places on the basis of these refinement studies and global orthogonal collocation computations in double precision.

Given errors in the derivative of the form $O(h^p)$ at the Gauss points the power p is obtained as the shape of the log-log plot of the magnitude of this error and mesh size h in Figure 1. The slopes for Gauss points 0.1,0.3,...,0.9 are, respectively, 2.0,2.0,1.8,1.8, which confirms the $O(h^2)$ superconvergence properties. The error in the solution at these points yields log-log curves with slopes 2.1,1.9,1.9,2.0,2.0 determined in like manner. Similar results are obtained with higher-degree elements (quadratics, cubics, ...).

Table 1. Convergence and Superconvergence at Gauss Points

Number of Elements	Error	Location of Selected Gauss Points and Error Values				
		x = 0.1	x = 0.3	x = 0.5	x = 0.7	x = 0.9
5	e	3.508157E-3	1.569525E-4	7.312965E-4	6.915672E-4	3.165209E-4
	e'	2.649675E-2	9.602573E-3	3.5065215E-3	6.222325E-4	5.248005E-4
25	e	1.443765E-4	2.7465E-6	3.2163E-5	2.94962E-5	1.34464E-5
	e'	1.4134225E-3	4.07585E-3	1.446525E-4	2.54075E-5	2.275E-5
125	e	5.6475E-6	6.7E-8	1.304E-6	1.1857E-6	5.394E-7
	e'	5.66625E-5	1.6225E-6	5.775E-6	1.0875E-6	8.7500E-7
625	e	1.305E-7	3.25E-8	6.45E-8	5.02E-8	2.19E-8
	e'	1.625E-6	5.625E-7	2.5E-7	1.25E-7	6.25E-8

Using linear regression analysis we find the following equations relating h and $|e|$:

at x = 0.1: $\log|e| = 2.102511 \log h - .93301046$

$\log|e'| = 2.007724 \log h - .10722941$

at x = 0.3: $\log|e| = 1.8895 \log h - 2.8406$

$\log|e'| = 2.0168 \log h - .5876$

at x = 0.5: $\log|e| = 1.93933 \log h - 1.7871$

$\log|e'| = 1.9799 \log h - 1.074$

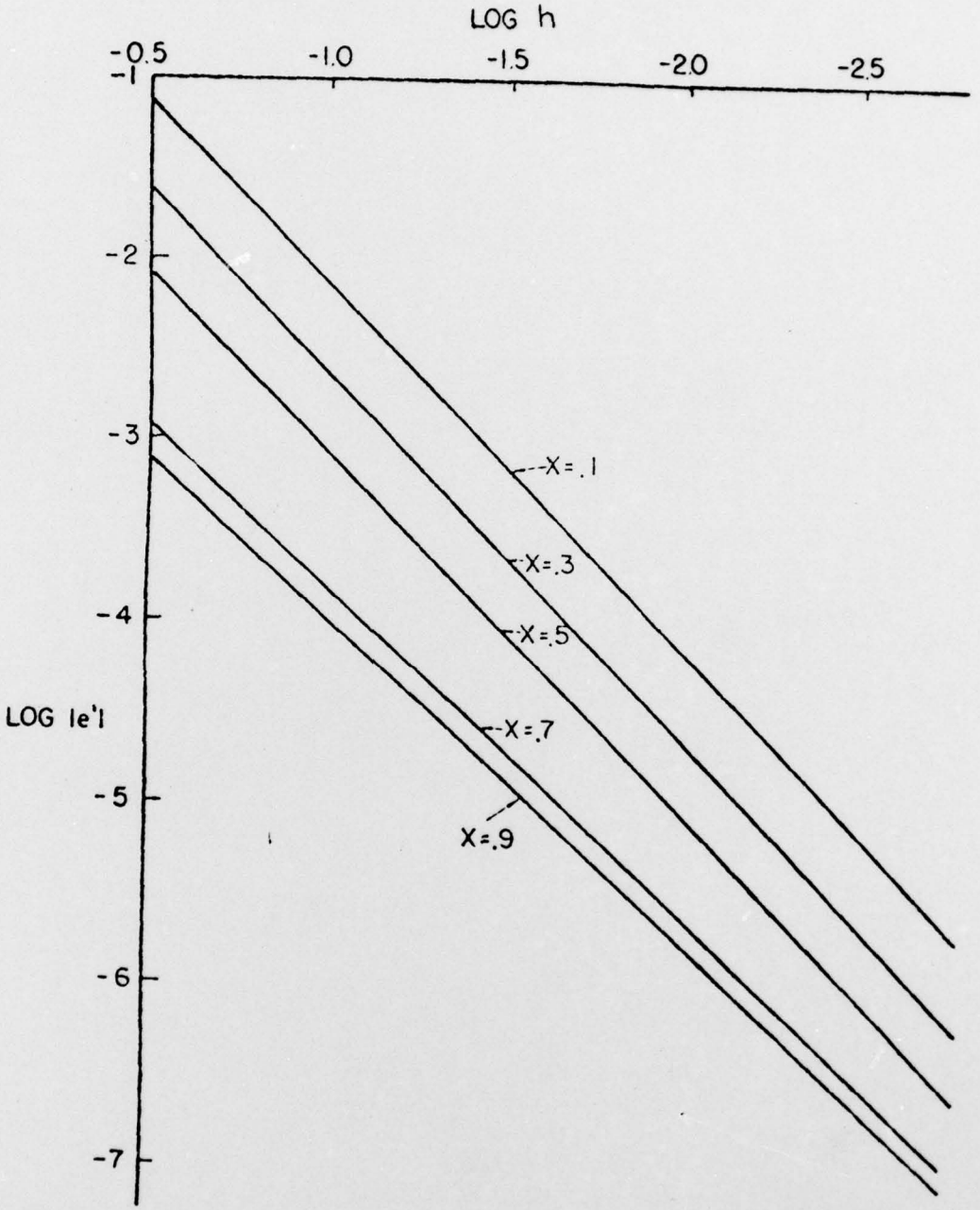

Figure 1. Error in derivative at the selected Gauss points 0.1,0.3,...,0.9. Slopes give the superconvergence rates $e' \sim O(h^2)$ for computations with linear elements here and in general $e' \sim O(h^{k+1})$ for elements of degree k.

Optimal Flux Computations

The boundary flux is of particular interest in practice as the governing equations in the pellet model are coupled to the mass and energy balances in the fluid phase through the boundary conditions. For our purposes an essentially exact flux dc/dx = 0.2834734796 accurate to all ten places is determined from a sequence of computations with uniform mesh refinements using quartic elements. This is used for comparison of computed fluxes using the standard approach and a new method recently proposed for which optimal estimates have been proven of linear problems [15].

The standard procedure for computing the boundary flux from the approximate solution is to differentiate the approximation polynomial on the last element and evaluate the resulting polynomial at the boundary node concerned. Since c(x) is $O(h^k)$ at x = 1 then c' is $O(h^{k-1})$. The new method is based on a quadrature algorithm on the last element.

The essential idea is to begin with the weighted-residual condition and integrate by parts as in the usual variational formulation, but by choice of a specific test (weight) function determine the flux from the element quadratures involved. Let $[x_{n-k}, x_n]$ denote the extreme element and apply the weighted-residual condition in equation (1), followed by integration by parts, to again obtain the variational statement in equation (3). The quantity of interest, c'(1), appears in the integrated boundary terms.

In the present instance we have computed an approximate solution c(x) and by simply setting v(0) = 0, v(1) = 1 in equation (3) we obtain an expression for c'(1),

$$c'(1) = \int_0^1 x^{n-1}(c'(x)v'(x) + f(c)v(x))dx \qquad (16)$$

More particularly, if $v(x)$ is chosen as the linear test function on the last element Ω_m,

$$v(x) = \begin{cases} 0 & , \quad x \in [0, x_{n-k}] \\ (x - x_{n-k})/h_m & , \quad x \in [x_{n-k}, 1] \end{cases} \tag{17}$$

Using the computed finite element solution for $c(x)$ in the integrand of (15), we need evaluate only simple quadratures on the last element to obtain the computed derivative,

$$\Gamma(1) = \frac{1}{h_m} \int_{x_{n-k}}^{1} x^{a-1} c'(x) dx + \int_{x_{n-k}}^{1} x^{a-1} f(c) v(x) dx \tag{18}$$

In linear problems if $c(x)$ has $(t+1)$ square-integrable derivatives (to be precise, $c \in H^{t+1}(\Omega) \cap H_0^1(\Omega)$ with H^{t+1}, H_0^1 representing standard Hilbert spaces [18]) then the error in Γ is $O(h^{t+k})$ where k is the degree of the element polynomial. The formulation is easily modified to yield the flux at an arbitrary node or any point $\hat{x}$ in $[0,1]$.

The formula (18) is used in the pellet problem to compute the boundary flux and is compared with results obtained by the standard approach. Uniform mesh refinements from 2 to 32 elements are employed for linear and quadratic elements in the comparison. In Table 2 errors in the boundary flux (E_F) for each of these cases are examined. The new scheme for computing boundary flux is evidently superior: for example, computing on a mesh of 16 quartic elements, we obtain 4 place accuracy using the standard method and 8 places with the quadrature calculations.

Table 2. Error in Computed Boundary Flux

		$E_F^{(1)} = \tilde{c}'(1)-c'(1)$	$E_F^{(2)} = \Gamma(1)-c'(1)$
Linear Elements	2	-2.580325850E-2	-7.009257E-4
	4	-1.20184279E-2	-2.604545E-4
	8	-5.3766312E-3	-7.26186E-5
	16	-2.4967754E-3	-1.87041E-5
	32	-1.1950125E-3	-4.713 E-6
Quadratic Elements	2	6.9828196E-3	-5.0954E-5
	4	1.9441702E-3	-3.4761E-6
	8	4.938324E-4	-2.225 E-7
	16	1.234531E-4	-1.39 E-8
	32	3.08068 E-5	8.6 E-9

The rates for this nonlinear singular problem are consistent with those predicted for linear problems. Again, a log-log plot of the magnitude of the error in boundary flux against mesh size h determines the experimental rate of convergence for $\Gamma(1)$. The rates (p) are the computed slopes of the linear regression curves in Figure 2: linears, p = 1.97, (2); quadratics, p = 3.9, (4). Corresponding computed rates for the standard method are 1.11,(1), and 1.96,(2), respectively. The conclusion concerning rates for elements of degree k is that differentiation produces fluxes of accuracy $O(h^k)$ while the optimal result $O(h^{2k})$ is obtained using the new quadrature scheme. The implications for nonlinear computations, especially if the pellet problem is to be solved numerous times for flux or effectiveness factor

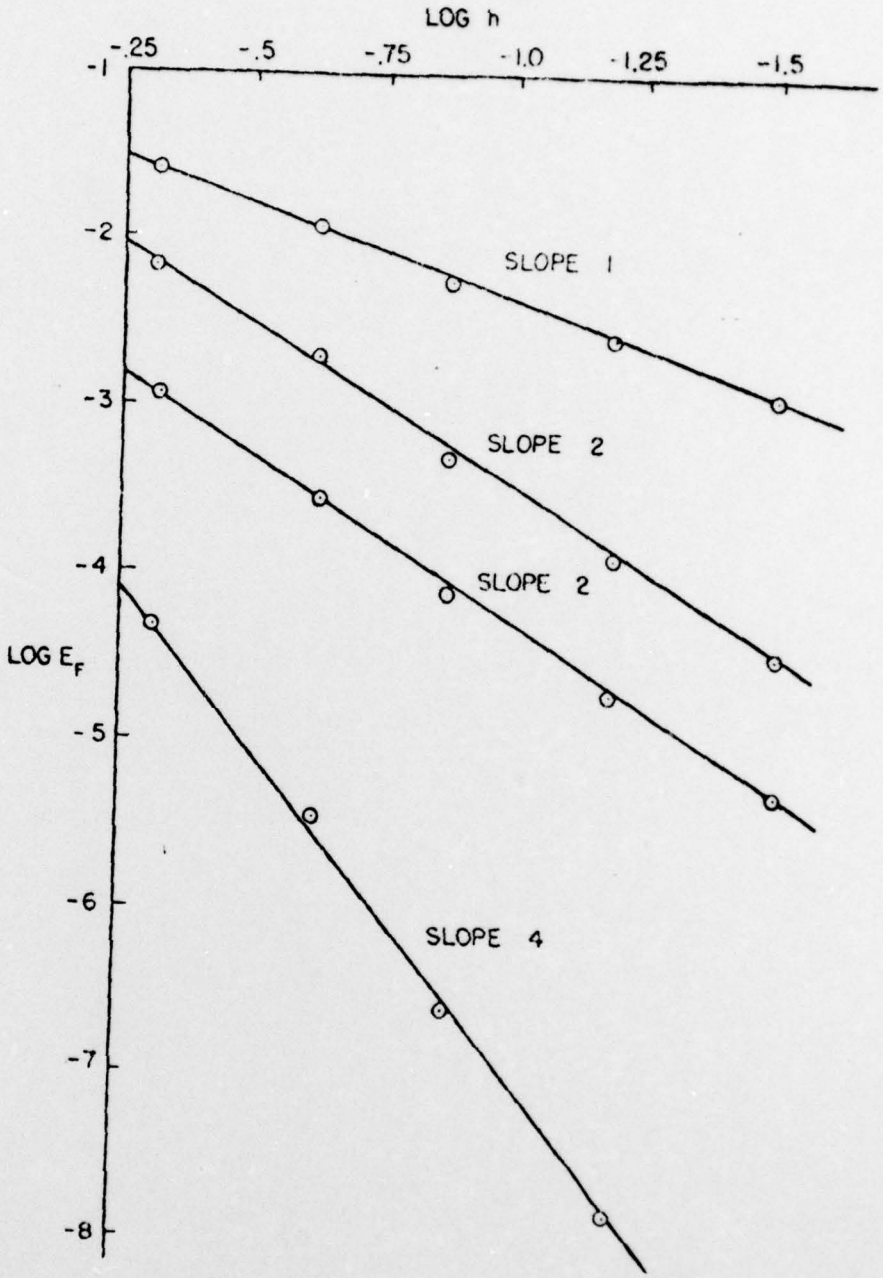

Figure 2. Error in boundary flux for pellet problem showing rates (slopes) for differentiation formula and new quadrature formula.

calculations, are evident. Since the work estimates for nonlinear solution are dramatically reduced if a coarser mesh can be used, fluxes of a desired accuracy can be computed much more efficiently using the quadrature result. For example, a flux computed by differentiation from an approximate solution of 32 quadratic elements (65 nodes) is less accurate than the new flux computed from a mesh of 2 quadratics (5 nodes). The respective computation times (using an efficient block diagonal-solver at each iteration to solve for c(x) differ by a factor of approximately 16.

Computational Aspects

A few brief remarks concerning computational details conclude this segment of the investigation. The design of the finite element program is based largely on that in reference [7] for the C^1 orthogonal collocation technique and is described there in some detail. Accordingly, only the main distinctions will be noted here.

The collocation technique leads to non-symmetric coefficient matrices for the Picard successive approximation systems and to a non-symmetric Jacobian in the Newton iteration necessitating non-symmetric system solvers for each linear iteration. In the Galerkin analysis for the stated class of self-adjoint differential equations, the finite element systems are symmetric. More efficient sparse elimination methods may be applied here and special iterative methods are also applicable [20,21].

The sparse matrices again have a block-diagonal structure each block being of size $(k+1) \times (k+1)$, where $k+1$ denotes the number of nodes in element e. This structure can be exploited to economize both storage and solution as described for the finite element collocation method. The special quadratures for optimal flux computations can be carried out using the basic Gaussian quadrature routines implemented for calculating the element matrix contributions to the (Galerkin) finite element system.

Part II. COLLOCATION-GALERKIN METHOD, JACOBI POINTS, AND FLUX CALCULATION

C^0-Collocation-Galerkin Method

Finite element collocation methods remove the necessity for element quadrature but require smoother bases. This smoothness condition becomes more prohibitive in higher dimensions. Even for the one-dimensional pellet models of interest here, there are situations such as those associated with layers and discontinuities where the less smooth C^0 Galerkin methods are more appropriate. As the terminology suggests, the C^0-Collocation-Galerkin method combines features of both collocation and Galerkin finite element methods. The main theoretical foundations and error estimates for linear and nonlinear problems are described in references [15], [16], and [18].

Qualitatively, the method is more like the C^1 collocation scheme. On any element of degree $k \geq 2$ the residual is collocated at k-1 interior points. Rather than enforce continuity of the derivative at interface nodes between elements, we require that a Galerkin projection for the variational problem hold there. Specifically, at the interface the nodal equation arises from a Galerkin projection of the residual with a test function that is only piecewise linear on the patch associated with the interface node.

To formulate the method return to the variational statement presented in equation (3),

$$- \int_0^1 x^{a-1}(c'(x)v'(x) + f(c)v)dx + x^{a-1}c'(x)v(x)\Big|_0^1 = 0 \qquad (19)$$

Define a partition of m elements and a C^0 Lagrange basis as in the Galerkin method of Part I so that

$$c(x) = \sum_{j=1}^{n} c_j \phi_j(x) \quad . \qquad (20)$$

where the basis $\{\phi_j(x)\}$, $j = 1,\ldots,n$ are again piecewise-polynomial patch functions identified with the nodes j. As usual, on element e,

$$c_e(x) = \sum_{j=1}^{k+1} c_j \ell_j^{(e)}(x) \tag{21}$$

where $\{\ell_j^{(e)}(x)\}$ are the Lagrange polynomials and here c_j are local (element) values of $c_e(x)$.

For test functions we select piecewise linear "hat" functions $\{\hat{p}_r(x)\}$, where {r} are the interface nodes. Setting $v(x) = \hat{p}_r(x)$ and using the approximation (20) in the variational statement (19), we obtain a set of m+1 finite element equations associated with the interface nodes and boundary nodes and of the form

$$\sum_{j=1}^{n}\left(\int_0^1 x^{a-1}\hat{p}_r'\phi_j' dx\right)c_j + \int_0^1 x^{a-1}\hat{p}_r(x)f(c)dx + x^{a-1}c'(x)v(x)\Big|_0^1 = 0 \tag{22}$$

the boundary conditions being included as in the Galerkin formulation. On element e, $\hat{p}_r(x) \equiv \hat{\ell}_r(x)$ and is linear, so that the element contribution to interface equation (22) is

$$g_r^{(e)}(\underset{\sim}{c}) = \frac{\pm 1}{h_e}\sum_{j=1}^{k+1}\left(\int_{\Omega_e} x^{a-1}\ell_j'(x)dx\right)c_j + \int_{\Omega_e} x^{a-1}\hat{\ell}_r(x)f(c)dx \tag{23}$$

The remaining interior collocation equations may be derived from equation (19). Since the element basis is C^∞ in the open interior of each element, we may reform the element residuals by integrating by parts in (19) to obtain

$$\int_{\Omega_e}\{x^{a-1}c')' - f(c)\}v\,dx = 0 \quad . \tag{24}$$

for test functions satisfying $v = 0$ at the end nodes of each element. Introduce delta function distributions for $v(x)$ to collocate the differential equation at k-1 points $\{x_p\}$ in the interior of each element,

$$\sum_{j=1}^{k+1} (x_p^{a-1} \ell_j'(x_p))' c_j - f(c) = 0 \quad , \; p = 1,\ldots,k-1 \qquad (25)$$

The appropriate collocation points for optimal accuracy are the Jacobi points in the element. Let $\{\alpha_j\}$, $j = 1,\ldots,k-1$ be the set of Jacobi points on interval $I = [0,1]$ and w_j the Jacobi weights defined by the quadrature formula

$$\int_I x(1-x)p\,dx = \sum_{j=1}^{k-1} \alpha_j(1-\alpha_j)p(\alpha_j)w_j \qquad (26)$$

for $p(x) \in P_{2r-3}(I)$, the set of polynomials of degree 2r-3 on I. Then on element r, the collocation points are located at

$$\alpha_{rj} = x_r + h_r\alpha_j \quad , \quad r = 1,\ldots,m;\; j = 1,\ldots,k-1 \qquad (27)$$

In [18] we demonstrate that for the linear problem the numerical solution is essentially exact at the nodes. Very accurate flux computations can be made using the quadrature procedure of equation (18). For the linear problem optimal estimates

$$|e(x_j)| = O(h^{2r}) \quad \text{and} \quad |e'(x_j)| = O(h^{2r}) \qquad (28)$$

are obtained when the flux is computed in this manner. The theoretical estimates for the nonlinear problem are developed in [16].

Flux Computation and Jacobi Points

We return to the catalyst pellet problem and examine the alternative flux techniques, again comparing computed values of the boundary flux. The numerical studies are designed to demonstrate the theoretical results stated above concerning use of the Jacobi points as collocation points and also the quadrature rule for flux computation. Again, $f(c) = \phi^2 c \exp[\gamma(1-1/T)]$, $T = 1 + \beta - \beta c$ and $c'(0) = 0$, $c(1) = 1$ are prescribed. The reaction parameters for this comparison study are $\phi = .5$, $\gamma = 18$ and $\beta = .3$.

In Table 3 the error in the boundary flux is given for solutions computed on meshes of 2, 4 and 8 quartic elements. The derivative $\Gamma(1)$ is computed by the quadrature formula using a finite element solution obtained by collocation at the Jacobi points. The derivative $\hat{c}'(1)$ is computed directly and in the table we demonstrate the relative accuracy here for solutions obtained by collocating at the Jacobi and Gauss points, respectively. There is a modest improvement (about one decimal place) if we compute the derivative directly from a collocation solution at the Jacobi rather than Gauss points. If in addition the quadrature technique is utilized, two or three further decimal places are obtained.

Table 3. Derivative accuracy using quadrature and Jacobi points.

Mesh	Jacobi Points		Gauss Points
(h^{-1})	$\lvert\Gamma - c'(1)\rvert$	$\lvert\hat{c}'(1) - c'(1)\rvert$	$\lvert\hat{c}'(1) - c'(1)\rvert$
2	2.1×10^{-8}	3.7×10^{-6}	1.0×10^{-5}
4	2.0×10^{-9}	2.2×10^{-6}	3.0×10^{-6}
8	3.0×10^{-9}	1.6×10^{-8}	8.0×10^{-7}

These results are also borne out in Table 4 where errors in the flux are determined from solutions on meshes of 2, 4, 8 and 16 cubic elements. The solutions are obtained by collocation at the Jacobi points. From a log-log plot of error and mesh size h we obtain $|\hat{c}'(1) - c'(1)| \sim O(h^{3.4}) \simeq O(h^{4})$, $k+1 = 4$ and $|\Gamma(1) - c'(1)| \sim O(h^{8})$.

Table 4. Boundary flux comparison for quadrature approach.

Mesh (h^{-1})	$\lvert\Gamma - c'(1)\rvert$	$\lvert\hat{c}'(1) - c'(1)\rvert$
2	5.9×10^{-9}	4.3×10^{-5}
4	2.7×10^{-9}	3.7×10^{-6}
8	1.8×10^{-10}	3.8×10^{-7}
16	1.2×10^{-11}	3.9×10^{-8}

Remark

The smoother C^1 approximations used in finite element collocation impose a quasi-uniformity requirement on nonuniform meshes encountered in practice. This restriction on the mesh does not apply to the C^0-Collocation-Galerkin procedure. The C^0 methods are, consequently, better suited to implementation in programs that incorporate automated mesh-refinement strategies. This latter consideration is particularly important in nonlinear boundary-layer problems corresponding to pellet models with large Thiele modulus [22].

Acknowledgement

This research has been supported in part by the Office of Naval Research Grant N00014-78-C-0550.

REFERENCES

1. Bird, R. B., Stewart, W. E. and Lightfoot, E. N.: Transport Phenomena, Wiley, New York, 1960.

2. Petersen, E. E.: Chemical Reaction Analysis, Prentice-Hall, New Jersey, 1965.

3. Aris, R.: The Mathematical Theory of Diffusion and Reaction in Permeable Catalysts, Clarinden Press, Oxford, 1975.

4. Finlayson, B. A.: The Method of Weighted Residuals and Variational Principles, Academic Press, New York, 1972.

5. Villadsen, J. and Michelsen, M. L.: Solution of Differential Equation Models by Polynomial Approximation, Prentice-Hall, New Jersey, 1978.

6. Paterson, W. R. and Cresswell, D. L.: Chem. Engng. Sci., 1971, 26, 605-616.

7. Carey, G. F. and Finlayson, B. A.: Chem. Engng. Sci., 1975, 30, 587-596.

8. Ciarlet, P. G., Schultz, M. H. and Varga, R. S.: Num. Math., 1967, 9, 394-430.

9. Schultz, M. H.: Spline Analysis, Prentice-Hall, New Jersey, 1973.

10. Fairweather, G.: Finite Element Galerkin Methods for Differential Equations, Dekker, 1978.

11. Martin, H. C. and Carey, G. F.: Introduction to Finite Element Analysis, McGraw-Hill, New York, 1973.

12. Dupont, T.: SIAM J. Numer. Anal., 1976, 13, 362-368.

13. Douglas, J., Jr. and Dupont, T.: Math. Comp., 1973, 27, 17-28.

14. De Boor, C. and Swartz, B.: SIAM J. Numer. Anal., 1973, 10, 582-606.

15. Wheeler, M. F.: SIAM J. Numer. Anal., 1977, 14, 71-90.

16. Wheeler, M. F. and Carey, G. F.: SIAM J. Numer. Anal. (to be submitted).

17. Eisenstat, S. C., Schreiber, R. S. and Schultz, M. H.: Advances in Computer Methods for Partial Differential Equations II, S. Vichnevetsky (ed.), IMACS (AICA) Publ., 1977.

18. Showalter, R.: Hilbert Space Theory and Partial Differential Equations, Pitnam, 1977.

19. Carey, G. F. and Wheeler, M. F.: Numerical Solution of Ordinary Differential Equations, B. Childs (ed.), Springer Lecture Notes in Computation, 1979 (in press).

20. Young, D. M., Jr.: Iterative Solution of Large Linear Systems, Academic Press, New York, 1971.

21. Carey, G. F. and Humphrey, D.: Numerical Solution of Ordinary Differential Equations, B. Childs (ed.), Springer Lecture Notes in Computation, 1979.

22. Wheeler, M. F.: SIAM J. Numer. Anal., 1974, pp. 764-768.

SECURITY CLASSIFICATION OF THIS PAGE (When Data Entered)

REPORT DOCUMENTATION PAGE

READ INSTRUCTIONS BEFORE COMPLETING FORM

1. REPORT NUMBER: TR-2
2. GOVT ACCESSION NO.
3. RECIPIENT'S CATALOG NUMBER

4. TITLE (and Subtitle): Galerkin and Collocation-Galerkin Methods with Superconvergence and Optimal Fluxes.

5. TYPE OF REPORT & PERIOD COVERED: Technical Report

6. PERFORMING ORG. REPORT NUMBER: TR-1, TR-2

7. AUTHOR(s): G. F. Carey, D. Humphrey, M. F. Wheeler

8. CONTRACT OR GRANT NUMBER(s): N00014-78-C-0550

9. PERFORMING ORGANIZATION NAME AND ADDRESS:
Texas Institute for Computational Mechanics
University of Texas at Austin
Austin, Texas 78712

10. PROGRAM ELEMENT, PROJECT, TASK AREA & WORK UNIT NUMBERS: NR064-478

11. CONTROLLING OFFICE NAME AND ADDRESS:
Office of Naval Research
Arlington, Virginia 22217

12. REPORT DATE: June 1979

13. NUMBER OF PAGES: 24

14. MONITORING AGENCY NAME & ADDRESS (if different from Controlling Office): 29p.

15. SECURITY CLASS. (of this report): Unclassified

15a. DECLASSIFICATION/DOWNGRADING SCHEDULE

16. DISTRIBUTION STATEMENT (of this Report): Unlimited

AD69830

DISTRIBUTION STATEMENT A
Approved for public release
Distribution Unlimited

17. DISTRIBUTION STATEMENT (of the abstract entered in Block 20, if different from Report)

18. SUPPLEMENTARY NOTES

19. KEY WORDS (Continue on reverse side if necessary and identify by block number)
finite elements, superconvergence, flux calculations, collocation-Galerkin

20. ABSTRACT (Continue on reverse side if necessary and identify by block number)
Finite element methods are formulated and examined for Galerkin and collocation schemes and a mixed collocation-Galerkin finite element method. Superconvergence at special points is investigated and a new method for calculating optimal derivatives such as fluxes or stresses in typical applications is described and implemented for an example problem.

408 958

DD FORM 1 JAN 73 1473 EDITION OF 1 NOV 65 IS OBSOLETE
S/N 0102-014-6601

Unclassified
SECURITY CLASSIFICATION OF THIS PAGE (When Data Entered)